Electronic Supplementary Material (ESI) for Soft Matter.

Supporting Information

Protonation induced pH increase at the tri-block copolymer micelle interface for transient membrane permeability at neutral pH

Yeasmin Sarkar,[a] Snigdha Roy,[a] Rini Majumder,[a] Sanju Das,[a,b] Dixit V. Bhalani,[c] Ambarish Ray,[b] Suresh Kumar Jewrajka[c] and Partha Pratim Parui*,[a]

Contents

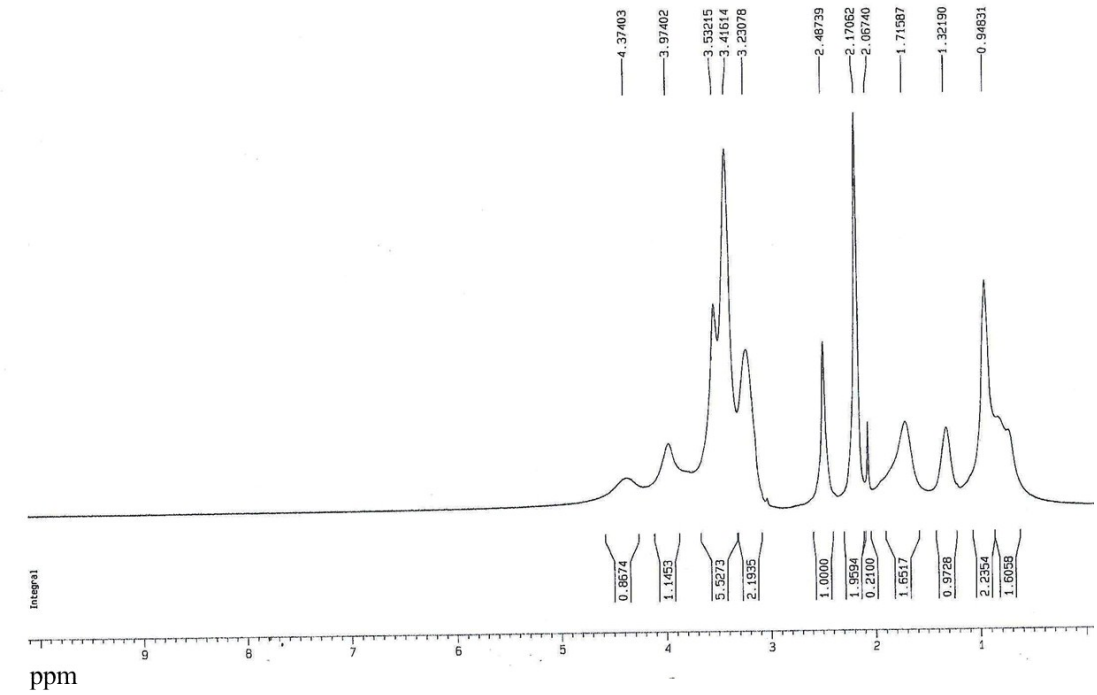

Fig. S1. ^{1}H-NMR spectrum of TBP in DMSO-d_6.

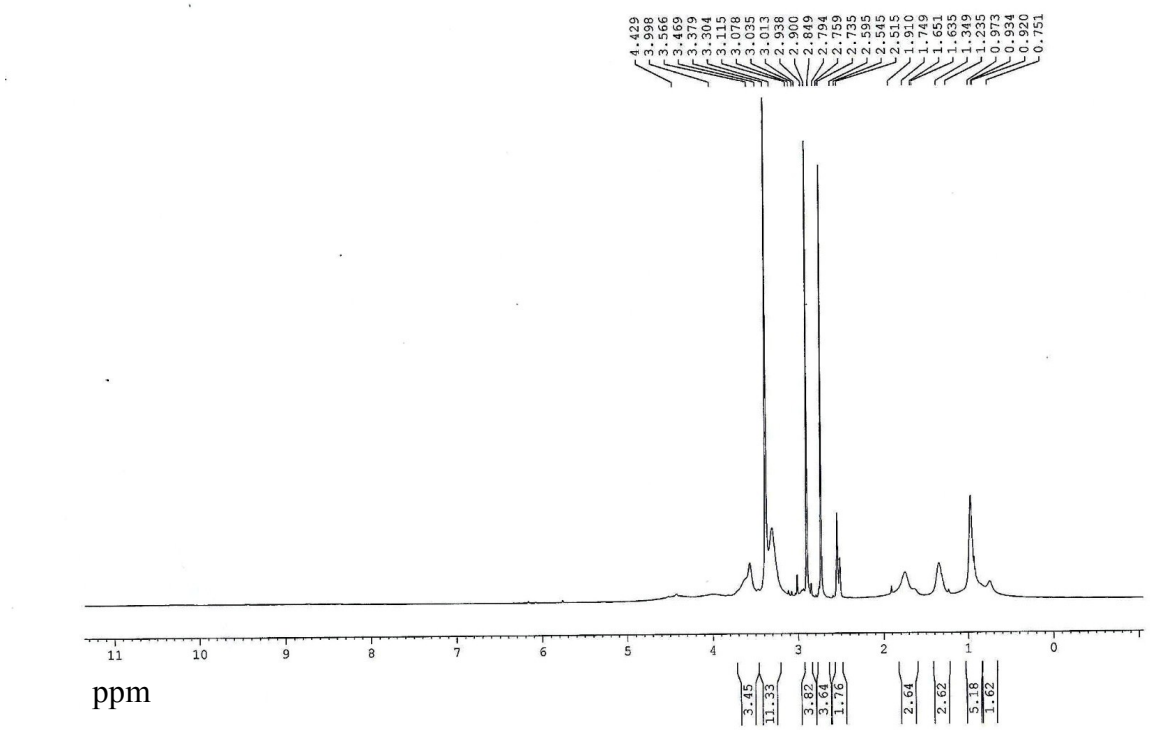

Fig. S2. ^{1}H-NMR spectrum of q-TBP in DMSO-d_6.

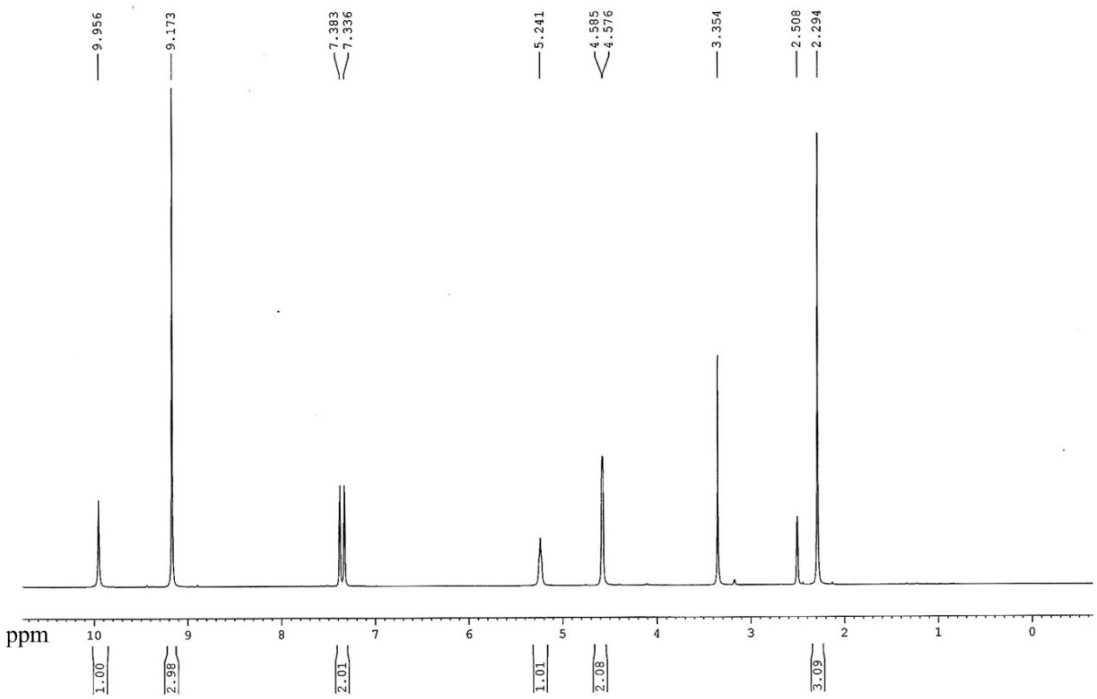

Fig. S3. ^{1}H-NMR spectrum of MSB in DMSO-d_6.

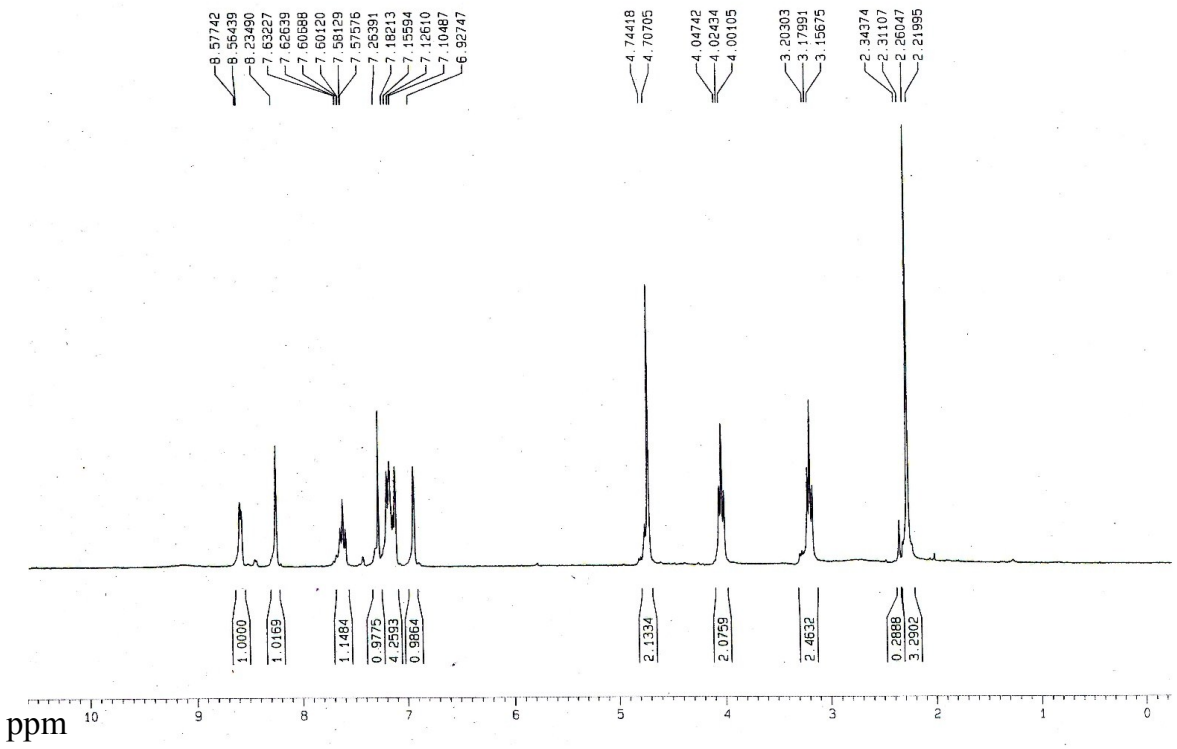

Fig. S4. ^{1}H-NMR spectrum of PMP in DMSO-d_6.

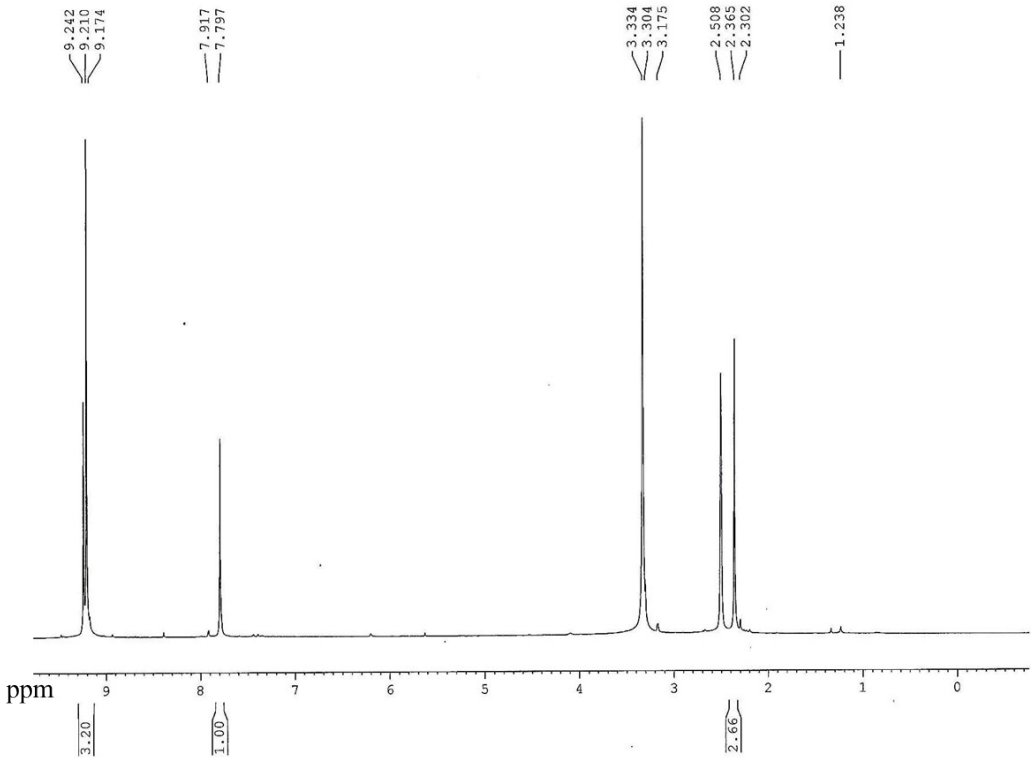

Fig. S5. ^{1}H-NMR spectrum of DSB in DMSO-d_6.

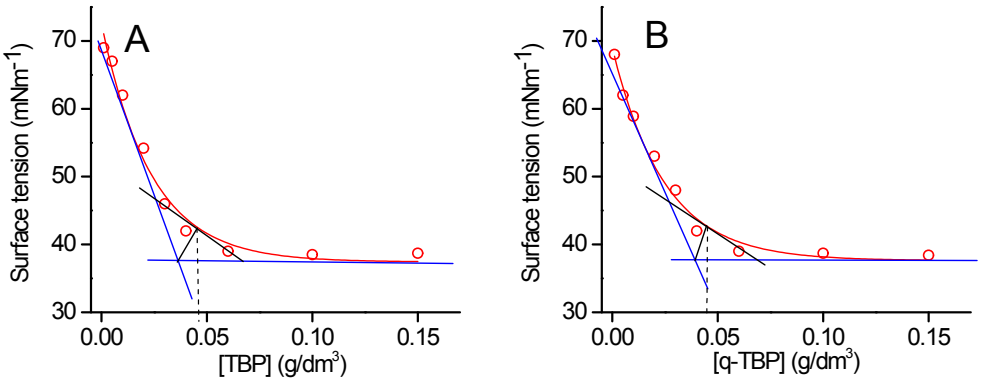

Fig. S6. (A) TBP and (B) q-TBP concentration dependent surface tension are plotted for the determination of critical micelle concentration (cmc).

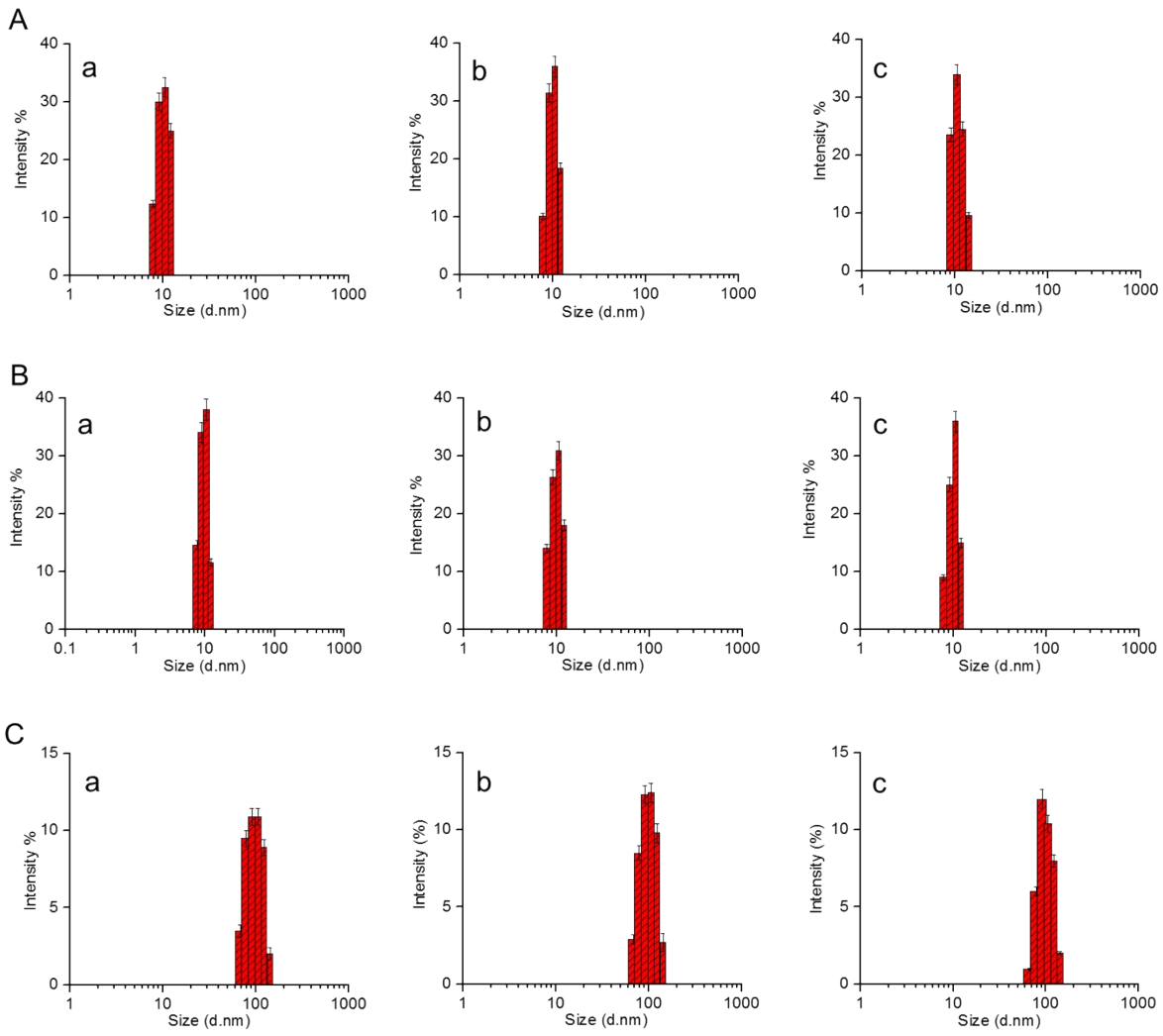

Fig. S7. DLS measurement showing particle size distribution profile of (A) TBP (1 g/dm^3) micelles, (B) q-TBP (1 g/dm^3) micelles, and (C) DOPC/DMPG (1:1) LUV (total lipids, 50 μM) at different pH: (a) 4.5, (b) 7.0 and (c) 9.0. Each of these spectra is an average of 48 scan. Standard deviations for measurements taken from five independent experiments are depicted by error bars.

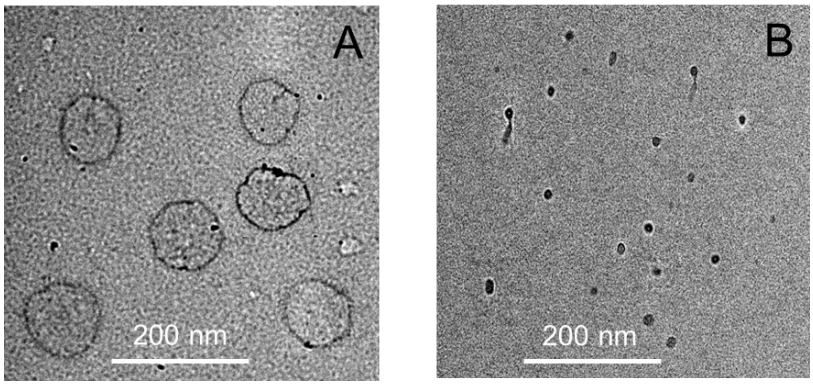

Fig. S8. Cryo-TEM image of (A) DOPC/DMPG LUV and (B) TBP micelle.

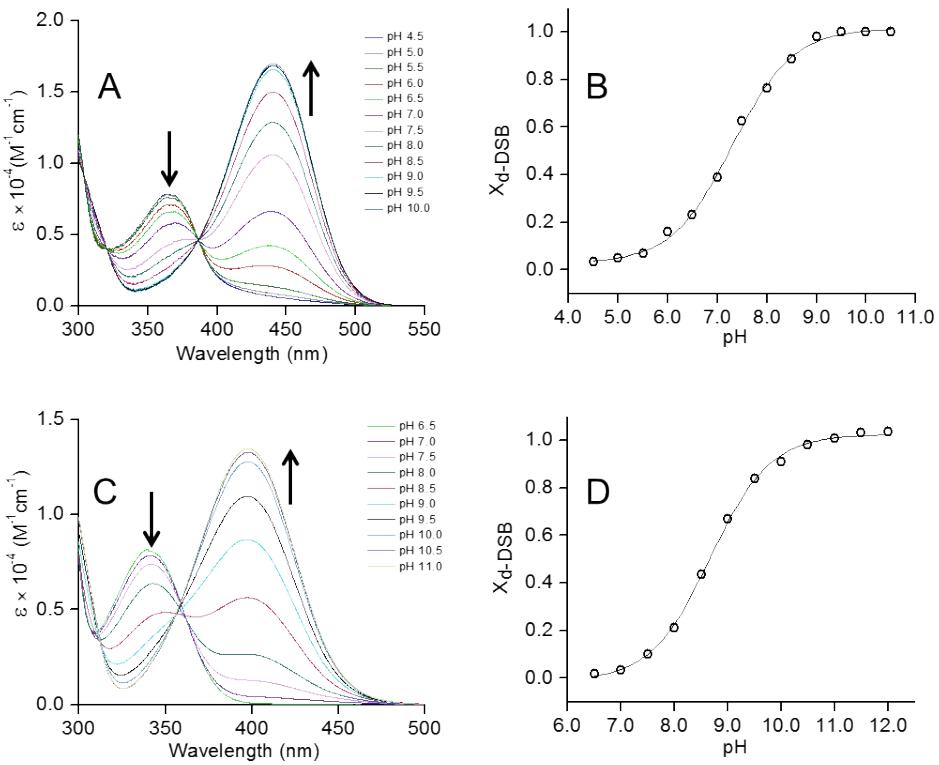

Fig. S9. pH dependent UV-vis absorption spectra of (A) DSB (5.0 μM) (pH: 4.5–10.0) and (C) MSB (5.0 μM) (pH: 6.5–11.0) in 10 mM different buffer medium: sodium citrate/sodium phosphate for pH 4.5−6.0, HEPES-NaOH for pH 6.5−8.0, carbonate/bi-carbonate for pH 9.0–12.0. The gradual increase or decrease of intensities with increasing pH are indicated by the arrows. pH dependent mole fraction (X) are plotted against different bulk pH of DSB (B) and MSB (D) deprotonated form (d-DSB, d-MSB). Each spectrum is normalized by dividing with the corresponding intensity at intensity-saturated pH value at maximum absorption wavelength (λ_{max}): (B) pH 10.0, and λ_{max}, 440nm for DSB; (D) pH, 11.5 and λ_{max}, 410 nm for MSB.

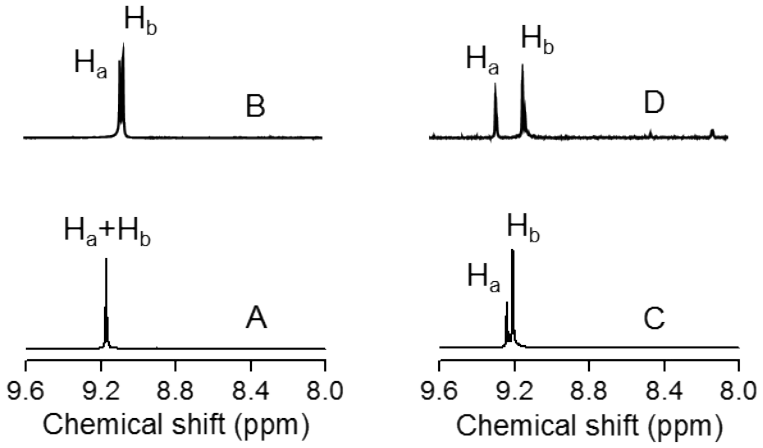

Fig. S10. ^{1}H NMR spectra (downfield region) of (A,B) MSB (2.0 mM) and (C,D) DSB (2.0 mM) in different solvents: (A,C), in DMSO-d_6; (B,D), in $MeOD_4$. (A,B) imine- and triazole-protons for MSB and DSB are labelled as H_a and H_b (shown in Fig. 1), respectively.

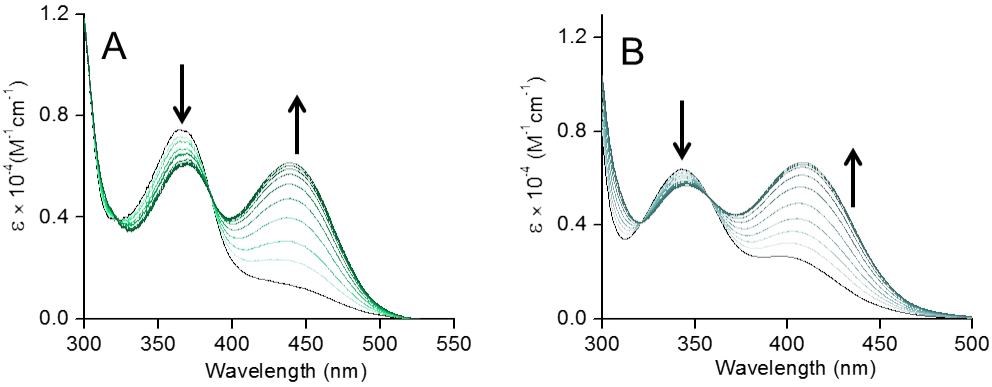

Figure S11. UV-vis absorption spectra in 20 mM different buffer in the presence of increasing concentration of TBP (0–1.0 g/dm^3) for (A) DSB (5.0 μM) at pH 5.5 in sodium citrate/sodium phosphate and (B) MSB (5.0 μM) in 10 mM HEPES-NaOH, pH 8.0. The spectra in absence of TBP are shown by black curve. The increasing or decreasing intensities with increasing concentration of TBP are indicated by arrows.

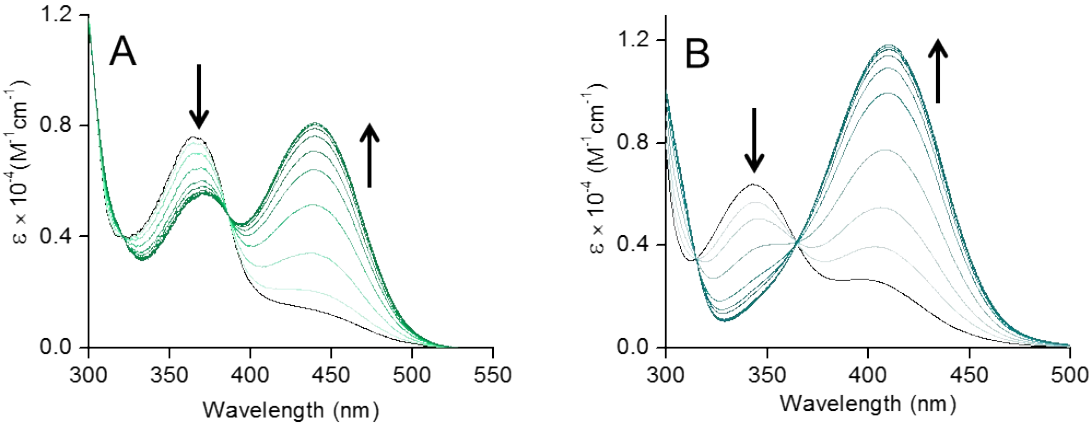

Figure S12. UV-vis absorption spectra in 10 mM different buffer in the presence of increasing concentration of q-TBP (0–1.0 g/dm^3) for (A) DSB (5.0 μM) in 10 mM sodium citrate/sodium phosphate buffer, pH 5.5 and (B) MSB (5.0 μM) in 10 mM HEPES-NaOH buffer, pH 8.0. The spectra in absence of q-TBP are shown by black curve. The increasing or decreasing intensities with increasing concentration of TBP are indicated by arrows.

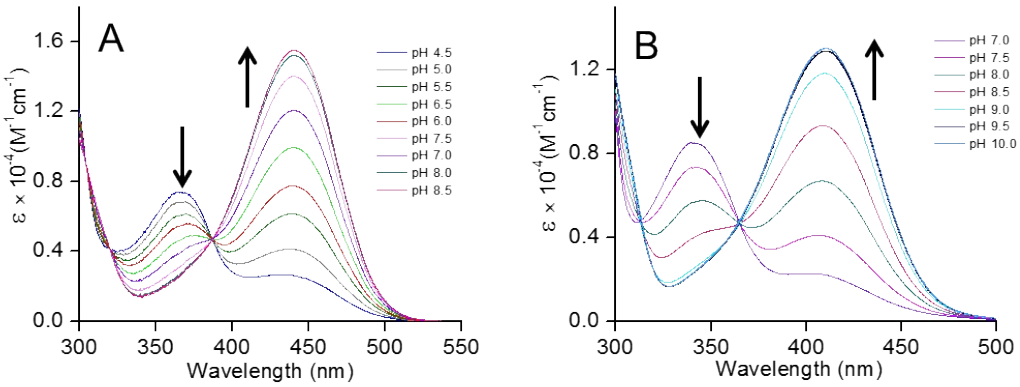

Figure S13. pH dependent UV-vis absorption spectra of (A) DSB (5.0 μM) (pH, 4.5–8.0) and (B) MSB (5.0 μM) (pH, 7.0–10.0) containing intensity-saturated concentrations of TBP (1.0 g/dm^3) in 10 mM different buffer medium: sodium citrate/sodium phosphate for pH 4.5−6.0, HEPES-NaOH for pH 6.5−8.0, carbonate/bi-carbonate for pH 9.0–12.0. The increasing or decreasing intensity with increasing pH are indicated by arrows.

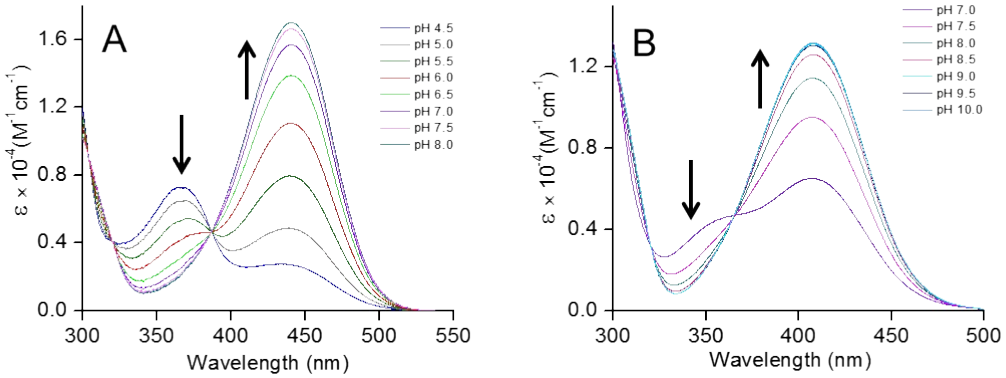

Figure S14. pH dependent UV-vis absorption spectra of (A) DSB (5.0 μM) (pH, 4.5–8.0) and (B) MSB (5.0 μM) (pH, 7.0–10.0) containing intensity-saturated concentrations of q-TBP (1.0 g/dm^3) in 10 mM different buffer medium: sodium citrate/sodium phosphate for pH 4.5−6.0, HEPES-NaOH for pH 6.5−8.0, carbonate/bi-carbonate for pH 9.0–12.0. The increasing or decreasing intensity with increasing pH are indicated by arrows.

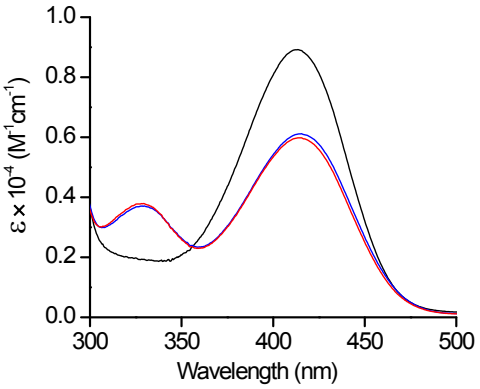

Fig. S15. UV-vis absorption spectra of PMP (5.0 μM) in the presence of of TBP (red) and q-TBP (blue) at their intensity-saturated concentration (1.0 g/dm^3) in 20 mM HEPES buffer, pH 7.0. The spectra in the absence of polymer micelle (black) is shown for comparison.

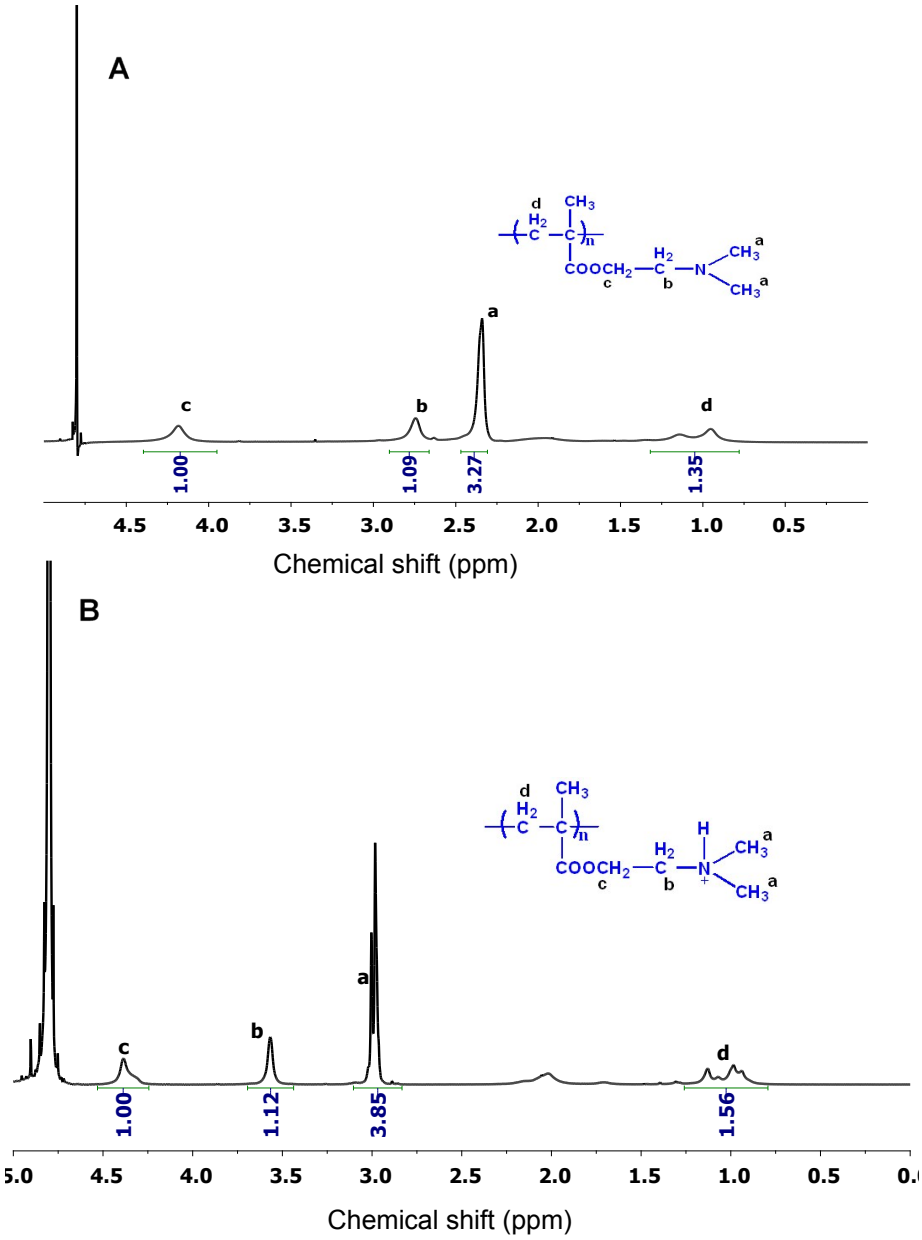

Fig. S16. pD dependent ^{1}H NMR spectra of homo-PDMA in D_2O: (A) pH 8.2 and (B) pH 6.0.

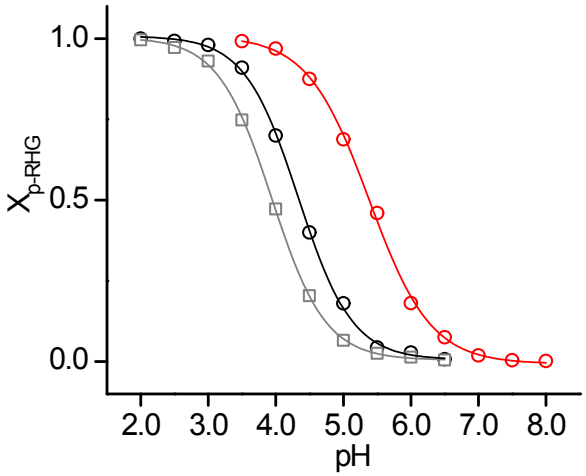

Fig. S17. The mole ratios of protonated form of glucose derivative of spiro-rhodamine molecule (RHG) ($X_{p\text{-}RHG}$) are plotted against bulk pH values in absence (black, circle) and the presence (red, circle) of DOPC:DMPG (1:1) LUV. The mole-ratio plots in 40 *wt*% ethanol containing 10 mM HEPES-NaOH buffer, pH 7.0 without polymer are also shown by gray. Each system are fitted with a single sigmoidal curve. The detail procedure is described in *Langmuir*, 2018, **34**, 6271-6284.

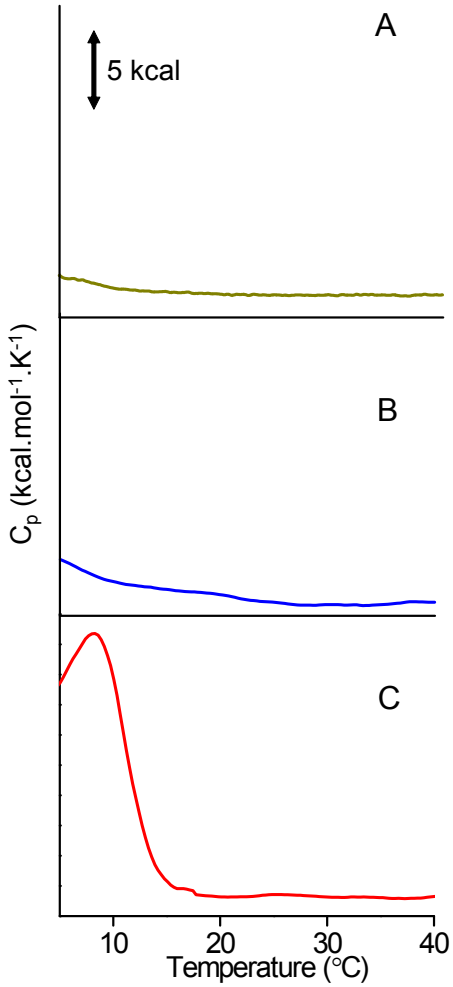

Fig. S18. Differential scanning calorimetry thermograms of DOPC/DMPG (1:1) LUVs (total lipids, 0.5 mM) in the (A) absence and (B) presence of DSB (2.5 μM) or (C) TBP micelle (0.5 g/dm^3) in 10 mM HEPES; pH, 7.0.

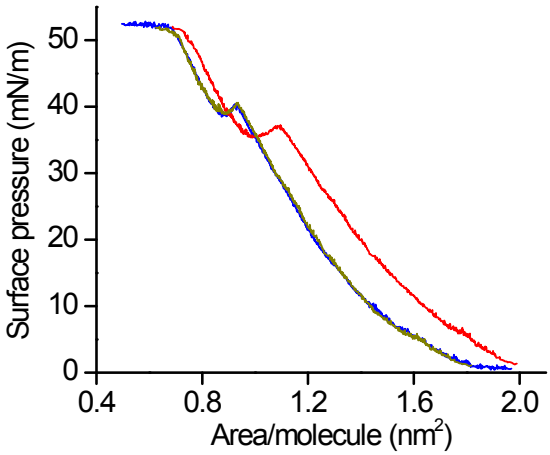

Fig. S19. Plots of monolayer pressure-area isotherm of DOPC/DMPG (1:1) in the absence (dark yellow) and presence of TBP (red) or DSB (blue).